

Magneto-ionic effect in CoFeB thin films with in-plane and perpendicular-to-plane magnetic anisotropy

L. Baldrati, A. J. Tan, M. Mann, R. Bertacco, and G. S. D. Beach

Citation: *Appl. Phys. Lett.* **110**, 012404 (2017); doi: 10.1063/1.4973475

View online: <http://dx.doi.org/10.1063/1.4973475>

View Table of Contents: <http://aip.scitation.org/toc/apl/110/1>

Published by the [American Institute of Physics](#)

Articles you may be interested in

[Magnetic tunnel junctions using perpendicularly magnetized synthetic antiferromagnetic reference layer for wide-dynamic-range magnetic sensors](#)

Applied Physics Letters **110**, 012401 (2017); 10.1063/1.4973462

[Influence of heavy metal materials on magnetic properties of Pt/Co/heavy metal tri-layered structures](#)

Applied Physics Letters **110**, 012405 (2017); 10.1063/1.4973477

[Enhancement of voltage-controlled magnetic anisotropy through precise control of Mg insertion thickness at CoFeB|MgO interface](#)

Applied Physics Letters **110**, 052401 (2017); 10.1063/1.4975160

[Observation of giant magnetoresistance in CoFeN/AIO_x/CoFeN magnetic tunneling junctions employing a nitrogen-doped amorphous CoFeN free layer electrode](#)

Applied Physics Letters **110**, 012402 (2017); 10.1063/1.4973407

[Electric field modulation of the non-linear areal magnetic anisotropy energy](#)

Applied Physics Letters **110**, 022405 (2017); 10.1063/1.4973700

[Impact of the interface quality of Pt/YIG\(111\) hybrids on their spin Hall magnetoresistance](#)

Applied Physics Letters **110**, 012403 (2017); 10.1063/1.4973460



Magneto-ionic effect in CoFeB thin films with in-plane and perpendicular-to-plane magnetic anisotropy

L. Baldrati,^{1,2,a)} A. J. Tan,² M. Mann,² R. Bertacco,^{1,3} and G. S. D. Beach²

¹*Dipartimento di Fisica, Politecnico di Milano, Milano 20133, Italy*

²*Department of Materials Science and Engineering, Massachusetts Institute of Technology, Cambridge, Massachusetts 02139, USA*

³*IFN-CNR, Milano 20133, Italy*

(Received 6 August 2016; accepted 18 December 2016; published online 5 January 2017)

The magneto-ionic effect is a promising method to control the magnetic properties electrically. Charged mobile oxygen ions can easily be driven by an electric field to modify the magnetic anisotropy of a ferromagnetic layer in contact with an ionic conductor in a solid-state device. In this paper, we report on the room temperature magneto-ionic modulation of the magnetic anisotropy of ultrathin CoFeB films in contact with a GdO_x layer, as probed by polar micro-Magneto Optical Kerr Effect during the application of a voltage across patterned capacitors. Both Pt/CoFeB/GdO_x films with perpendicular magnetic anisotropy and Ta/CoFeB/GdO_x films with uniaxial in-plane magnetic anisotropy in the as-grown state exhibit a sizable dependence of the magnetic anisotropy on the voltage (amplitude, polarity, and time) applied across the oxide. In Pt/CoFeB/GdO_x multilayers, it is possible to reorient the magnetic anisotropy from perpendicular-to-plane to in-plane, with a variation of the magnetic anisotropy energy greater than 0.2 mJ m⁻². As for Ta/CoFeB/GdO_x multilayers, magneto-ionic effects still lead to a sizable variation of the in-plane magnetic anisotropy, but the anisotropy axis remains in-plane. *Published by AIP Publishing.*
[\[http://dx.doi.org/10.1063/1.4973475\]](http://dx.doi.org/10.1063/1.4973475)

Voltage control of magnetism in metallic thin films has attracted great interest in the scientific community, both for fundamental and technological reasons. The idea of manipulating a parity-even time-odd vector (magnetization) by means of a parity-odd time-even vector (electric field) is very intriguing and challenging.^{1,2} On the other hand, the electric control of magnetic properties holds potential for solving the current bottleneck of spintronics and magnetic logic: the writing of a magnetic configuration in an energy efficient and scalable way.^{3,4} First demonstrations of the voltage control of magnetic properties in thin films were achieved in hybrid piezoelectric-metal systems, via inverse magnetostriction.^{5,6} A purely electric control of magnetic properties was then demonstrated in magnetic thin film immersed in an electrolyte, by the effect of the large electric field confined at the interface between the metal and the liquid.⁷ Recently, electric field effects on magnetic properties were demonstrated in all-solid-state devices, exploiting mechanisms such as interfacial hybridization induced by a change in electronic *d* orbital population, magneto-electric coupling in multiferroics and accumulation of charges induced by ferroelectric polarization in artificial multiferroics.^{8–13} On a parallel line, ion migration has been widely exploited in non-magnetic devices, e.g., made by an oxide layer sandwiched by two metallic layers, suitable for resistive switching technology.^{14,15} The magneto-ionic effect, i.e., the electric control of magnetic properties mediated by ion migration,^{16,17} is a physical phenomenon connecting these two fields. In this context, some of us recently proved that the voltage-driven migration of oxygen in the Pt/Co/

GdO_x system is able to dramatically modify the magnetic properties of the cobalt layer, changing the Magnetic Anisotropy Energy (MAE) at the interface by ~0.75 mJ m⁻² at room temperature.¹⁸ A more recent paper reported on voltage control of magnetism in Pt/Co/Gd₂O₃ by reversible oxidation at high temperature (200–260 °C), estimating a similar MAE variation (0.73 mJ m⁻²).¹⁹

In this paper, we report on the electric field control of the interface anisotropy mediated by magneto-ionic effects in a different system, Pt(Ta)/Co_{0.6}Fe_{0.2}B_{0.2}/GdO_x multilayers. At variance with previous works on magneto-ionic effects in Co thin films, here we use a CoFeB ferromagnetic layer. This choice is motivated by the technological relevance of this material, due to the record magnetoresistance obtained in CoFeB/MgO based tunneling junctions at room temperature, and its wide use in other fields such as magnonics and magnetic logic.^{20–23} As grown films of CoFeB on Pt display perpendicular to plane magnetic anisotropy (PMA), while those grown on Ta present conventional in-plane magnetic anisotropy (IMA). We show that the magnetic anisotropy of ultra-thin CoFeB films grown on top of Pt can be electrically reoriented from perpendicular-to-plane to in-plane and vice-versa, similarly to the case of Pt/Co/GdO_x.^{18,19} For CoFeB thin films grown on Ta, the switch between IMA and PMA cannot be achieved electrically, but a sizable variation of the CoFeB magnetic properties is still induced, as seen by the variation of the slope of the hard axis loops measured by polar magneto optical Kerr effect (MOKE).

In order to achieve magneto-ionic control of anisotropy in CoFeB, multilayers with structure sub//Ta(4)/Pt(10)/Co_{0.6}Fe_{0.2}B_{0.2}(0.7)/GdO_x(4) (CFB-Pt from now on) and

^{a)}Electronic mail: lorenzo.baldrati4@gmail.com

sub//Ta(4)/Co_{0.6}Fe_{0.2}B_{0.2}(0.9)/GdO_x(4) (CFB-Ta from now on) were sputter deposited on thermally oxidized silicon substrates (sub) with SiO₂ thickness of 50 nm. Thicknesses are expressed in nanometers. The growth was performed at room temperature by DC sputtering in Ar for all the layers except GdO_x, whose growth was carried out by reactive sputtering of a metallic Gd target in a mixed Ar and O₂ atmosphere. All layers were grown in a magnetic field (~ 10 mT) directed along the plane of the sample. In Figures 1(a) and 1(b) we show Vibrating Sample Magnetometry (VSM) measurements of as-grown multilayers at room temperature. CFB-Pt samples display a strong perpendicular magnetic anisotropy, while CFB-Ta ones have an in-plane magnetic anisotropy, thus underlying the predominant role of interfacial anisotropy induced by Pt to achieve PMA. As expected, we do not see secondary hysteresis loops coming from paramagnetic GdO_x. VSM measurements yield a saturation magnetization $M_S = 1080 \text{ kA m}^{-1}$ and $M_S = 850 \text{ kA m}^{-1}$ in the case of CFB-Pt and CFB-Ta, respectively. The M_S value found in CFB-Pt films is in agreement with the literature on CoFeB thin films, while the reduced value found in CFB-Ta films could be ascribed to a mild oxidation of the magnetic layer, probably driven by the gettering action of oxygen by the Ta layer underneath the ultrathin CoFeB layer.²⁴ Oxygen atoms may be incorporated in CoFeB either during its growth (due to presence of some residual oxygen atoms in the chamber which are captured by the Ta template) or also during the reactive sputtering of GdO_x, because of the permeability of the polycrystalline ultrathin CoFeB layer, which cannot completely passivate the Ta layer. As a matter of fact, a reduced M_S value was reported for CoFeB/Ta films grown in contact with other oxides.¹³ We have estimated the effective anisotropy constant in the virgin state of the samples using the formula

$$K_{\text{eff}} = (\mu_0 H_K M_S) / 2, \quad (1)$$

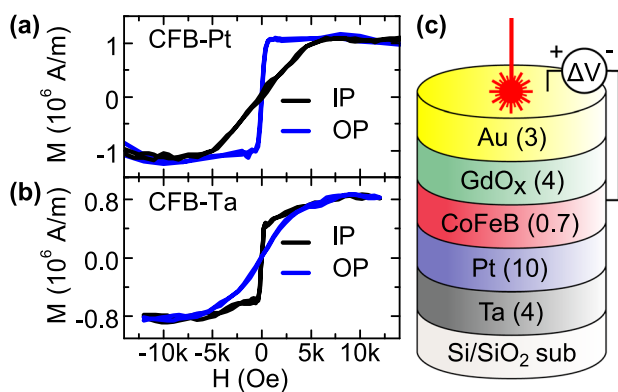


FIG. 1. (a) In-plane (IP) and Out-of-Plane (OP) Vibrating Sample Magnetometry (VSM) measurement of as-grown sub//Ta(4nm)/Pt(10)/Co_{0.6}Fe_{0.2}B_{0.2}(0.7)/GdO_x(4) unpatterned thin films (CFB-Pt), showing perpendicular magnetic anisotropy (PMA). (b) VSM of sub//Ta(4)/Co_{0.6}Fe_{0.2}B_{0.2}(0.9)/GdO_x(4) unpatterned thin films (CFB-Ta), showing in-plane magnetic anisotropy. (c) Scheme of the polar-MOKE measurement and CFB-Pt sample layout for measurements of the magneto-ionic effect in Pt/CoFeB/GdO_x perpendicularly magnetized capacitors. All thicknesses are expressed in nanometers. CFB-Ta does not have Pt in the stack. A red light laser is focused on top of the sample, while the polarization voltage ΔV is applied across the GdO_x layer. The convention for a positive voltage polarity is indicated.

where H_K is the saturation field along the hard axis. The effective magnetic anisotropy constant is $K_{\text{eff}} = 2.9 \times 10^5 \text{ J m}^{-3}$ in CFB(0.7 nm)-Pt and $K_{\text{eff}} = -1.6 \times 10^5 \text{ J m}^{-3}$ in CFB(0.9 nm)-Ta, where a positive sign indicates PMA. CFB-Ta presents a uniaxial magnetic anisotropy in the plane, whose easy axis direction is set by the small magnetic field applied during the growth. Noteworthy, in case of CFB-Ta, we were not able to drive the magnetic anisotropy out of the plane by *ex-situ* annealing, by contrast to what happens, e.g., in Ta/CoFeB/MgO or Ta/CoFeB/BaTiO₃.^{13,22} The difference in magnetic anisotropy between CoFeB grown on top of Pt and Ta may be attributed to the different hybridization at the interface and spin-orbit interaction of the two materials.²⁵ Other effects, such as strain or asymmetries in interfacial bonding, could also play a role.²⁶

The layout of the CFB-Pt patterned samples and the scheme of the measurement are shown in Figure 1(c). Circular thin gold contacts (3 nm thick and 100 μm wide) were fabricated on top of CFB-Pt and CFB-Ta samples by sputtering with shadow masks, providing an array of capacitors. We acquired polar micro-Magneto Optical Kerr Effect (μ -MOKE) hysteresis loops at normal incidence, during the application of a voltage across the oxide, in air at room temperature. A red laser of wavelength $\lambda = 655 \text{ nm}$ was focused to a spot dimension of $\sim 3 \mu\text{m}$ at the top of the patterned samples, passing through the gold contact and allowing to measure the CoFeB hysteresis loops with a sufficient signal/noise ratio, thanks to the transparency of GdO_x and the small thickness of the gold layer. The acquisition of each MOKE hysteresis loop took 200 ms and an average of 10 hysteresis loops was taken. In this configuration, MOKE probes only the magnetization component perpendicular to the plane of the sample, which direction is the easy axis in the as-grown CFB-Pt and the hard axis in as-grown CFB-Ta. No sizable contribution to the MOKE signal is expected from paramagnetic GdO_x at room temperature. Also supposing that oxygen migration leads to the formation of metallic Gd clusters, the Curie temperature (T_C) of bulk metallic Gd is 293.2 K (Ref. 27) and we expect an even lower T_C for clusters, so that the MOKE signal can be unambiguously attributed to CoFeB. From now on, a positive voltage corresponds to a positive voltage drop ΔV between the top (Au) and the bottom (CoFeB) electrode (see Figure 1(c)). Negatively charged oxygen ions (O^{2-}) are attracted toward the positive pole. Therefore, a sizable oxidation (reduction) of the CoFeB layer is expected for positive (negative) voltage ΔV applied across the capacitors. This is the main mechanism leading to magneto-ionic effects, as demonstrated by Transmission Electron Microscopy-Electron Energy Loss Spectroscopy and X-Ray Magnetic Circular Dichroism in previous studies on Cobalt.^{18,19} The electric resistance of the capacitors is only slightly altered upon application of voltages on the order of $\pm 2 \text{ V}$, from the $\text{G}\Omega$ to the $100 \text{ M}\Omega$ range; overall the GdO_x behaves as an insulator and most of the voltage drops across the GdO_x layer.

In Figures 2(a)–2(j), we present data obtained in the perpendicularly magnetized CFB-Pt sample as a function of the applied voltage ΔV . The initial state ($t = 0$) was prepared after a forming process, applying -2 V for $\sim 10 \text{ s}$ and then

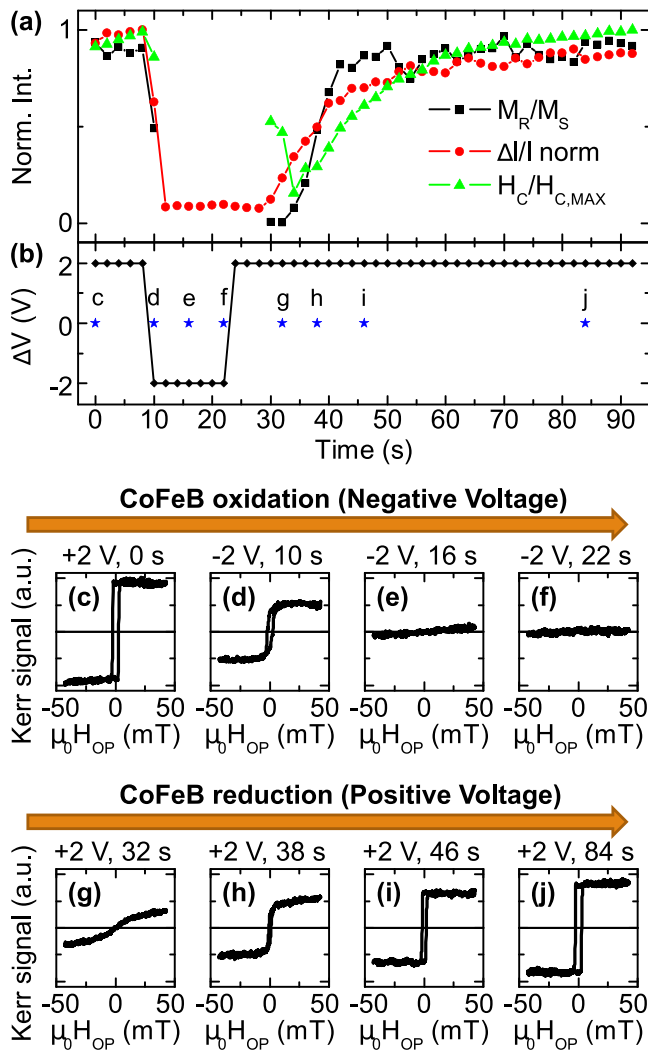


FIG. 2. (a) Time evolution of various parameters extracted by polar MOKE hysteresis loops: saturation magnetization M_R/M_S , coercive field H_C , and MOKE normalized signal intensity ($\Delta I/I$) in the presence of an applied potential. Note that the time scale is the same for panels (a) and (b). (b) Applied potential as a function of time. The blue stars on the time scale indicate the time of recording of selected MOKE loops shown in full details in panels (c)–(j). (c)–(j) Selected polar MOKE hysteresis loops of CFB-Pt sample, corresponding to measurements indicated in panel (b) by blue stars. The applied voltage ΔV and the starting time of the acquisition are reported at the top of each panel. (c)–(f) A negative applied voltage drives the oxygen in the CoFeB layer (oxygen enrichment). The anisotropy easy axis reorients from out of plane to in plane. (g)–(j) If the sign of the voltage is reversed, the oxygen is driven away from CoFeB (oxygen depletion) and the initial state can be restored.

+2 V for ~ 20 s. After this preparation, we found a steady state with a perpendicular easy axis, shown in Figure 2(c), having a coercive field $\mu_0 H_C$ of 2.5 mT and a remnant magnetization M_R/M_S approaching 100%. We then apply ($t = 10$ s) a negative gate voltage (-2 V), driving oxygen into the CoFeB magnetic layer. This results in a drop of the coercive field H_C , the remnant magnetization M_R/M_S and the MOKE signal $\Delta I/I$, calculated as the ratio of the magnetic signal amplitude to the average normalized intensity, as shown in Figures 2(a) and 2(b). The magnetic signal amplitude ΔI is defined as the difference between the maximum and minimum Kerr light intensity recorded by the photodetector during the magnetic field sweep. Note that only few seconds are required to reach a steady state in presence of a

negative gate voltage ΔV . The loops in Figures 2(d)–2(f) show a change in the shape of the hysteresis loops, which gradually becomes like hard-axis. This indicates a change from an out-of-plane to an in-plane magnetic easy axis, as previously demonstrated in a Pt/Co/GdO_x system.^{18,19} Finally, we apply a positive gate voltage ($t = 22$ s), so as to drive the oxygen out of the magnetic CoFeB layer and restore the initial state in terms of all the three parameters under study. This recovery process is presented in Figures 2(g)–2(j). The final loop in Figure 2(j) has a magnetic coercive field $\mu_0 H_C$ of 2.6 mT and M_R/M_S approximately equal to 100%, so that the parameters are the same as in the initial state of Figure 2(c). Both the magnitude of the variation of the magnetic properties and the timescale of the evolution point to an effect mediated by ion migration, instead of a pure magneto-electric effect induced by the electric field at the GdO_x/CoFeB interface. The excursion of the electric field at the surface of the CoFeB layer is approximately equal to $\pm 5 \times 10^8$ V/m, when reversing the bias from +2 V to -2 V. In case of systems directly controlled by an electric field, even for the prototypical case of CoFeB/MgO/CoFeB tunnel junctions, a field variation of this entity did not lead to a full reorientation of the magnetic easy axis, as that reported in the present paper.¹¹ Moreover, we observe a temporal evolution much slower than the one associated with the electric field only, which should be quasi-instantaneous. As a matter of fact, the behavior observed here is very similar to the one found in Pt/Co/GdO_x, which stems from the voltage controlled oxidation of the Co layer.¹⁸ Comparable results have been obtained on a similar CFB-Pt stack with a 0.9 nm thick CoFeB layer, thus indicating the robustness of the magneto-ionic coupling with respect to the thickness of the layer (see Figure S2 in the [supplementary material](#)). Note that the switching can be reversibly performed many times at low bias. If a high unipolar bias is applied for a long time, a permanent deterioration of the system is seen with appearance of some irreversibility (see Figure S3 in the [supplementary material](#)). The evolution for positive applied voltage is much slower, taking around 60 s to be completed, consistently with what was found in Co.^{18,19} Bi *et al.* suggested that this asymmetry in the evolution times may be related to the different CoO/Gd₂O₃ barrier between the oxidized and non-oxidized case.¹⁹ The fact that the process is slower for positive applied voltage is somehow counter-intuitive, since Gd₂O₃ is thermodynamically favored over the formation of any of the Co or Fe oxides.²⁸ A possible explanation is that, when a negative voltage is applied across the structure, an oxygen ion O^{2-} can easily move into the CoFeB layer, by creating a vacancy. On the contrary, if a positive voltage is applied, an oxygen ion O^{2-} cannot move in GdO_x, unless it annihilates a vacancy, which must migrate to the GdO_x/CoFeB interface. The migration of the ion and the vacancy to the same place is an additional step with associated energy barrier and characteristic diffusion time, which slows down the process. See the [supplementary material](#) for further details.

Since the magnetic anisotropy switches from perpendicular-to-plane to in-plane (implying a change of sign of the effective anisotropy constant), the variation of K_s is at least greater than the initial value. From the knowledge of the effective magnetic anisotropy constant K_{eff} of the virgin

state, as measured by VSM (see Fig. 1), we can set a lower limit of the interface magnetic anisotropy variation

$$\Delta K_s > K_{\text{eff}} t = 0.20 \text{ mJ/m}^2,$$

where t is the thickness of the CoFeB layer.

Magneto ionic effects have been investigated also in case of multilayers with in-plane anisotropy, by fabricating capacitors on the in-plane magnetized CFB-Ta sample, whose VSM is shown in Figure 1(b). The layout of the CFB-Ta patterned sample is similar to the CFB-Pt one shown in Figure 1(c), except for the absence of the Pt layer and a different nominal CoFeB thickness, which is 0.9 nm in this case. In Figure 3, we present selected polar MOKE loops acquired as a function of the voltage. The curves display no hysteresis and a linear behavior which is consistent with the VSM measurements performed in a wider range of magnetic field (see Figure 1), thus indicating a magnetic hard axis along the direction normal to the plane of the sample in the virgin state. The application of a gate voltage for a few seconds allows to change the slope measured in the MOKE hysteresis loops. The maximum slope we were able to achieve by a positive voltage was 4.2 times the slope of the virgin state, while the minimum slope, obtained by a negative voltage, was about 0.3 times that of the virgin state. Unfortunately, we could not measure by MOKE the saturation magnetization nor the variation of the anisotropy field (the electromagnet available on the setup was limited to 500 Oe); therefore, a quantitative determination of the magnetic anisotropy energy variation is prevented. Most probably, the increase in the slope in MOKE loops for positive voltage is partially due to the reduction of the CoFeB layer, which is expected to increase the saturation magnetization, and partially to the increase in the positive PMA contribution to the effective anisotropy constant K_{eff} , which is negative for in-plane anisotropy. According to the Stoner-Wohlfarth model, the slope of the loop measured along a hard-axis is given by $\mu_0 M_S^2 / (2|K_{\text{eff}}|)$, so that both an increase in M_S and a decrease in $|K_{\text{eff}}|$ can contribute to the variation seen in Fig. 3 between the black (as-grown) and red (+10 V) loops. The as-grown film appears oxidized, as confirmed by

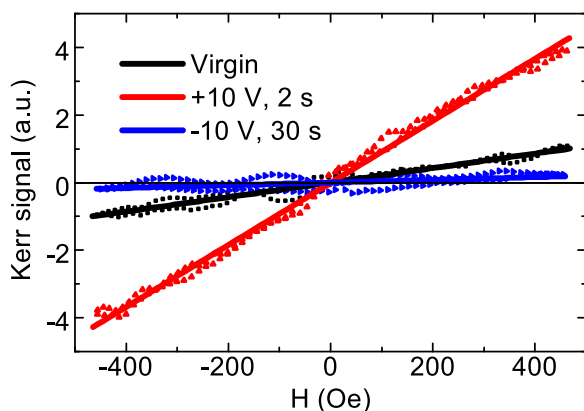


FIG. 3. Polar MOKE hysteresis loops of in-plane magnetized Ta/GdO_x/CoFeB films. The linear behavior corresponds to the central part of the curve measured in the out-of-plane configuration by VSM on the same sample before patterning, as shown Figure 1(c), where also the in-plane loop is reported. The continuous line is a fit of the experimental data and a positive voltage increases its slope by a factor 4.2, while a negative voltage sorts the opposite effect and the slope becomes 0.3 times the virgin.

the reduced saturation magnetization measured by VSM, so that the application of a positive voltage induces a partial reduction of the CoFeB layer. As previously reported for the Pt/Co/GdO_x system with PMA, the interfacial Co oxidation promotes PMA but an over-oxidation can drive the system into an easy-plane anisotropy state.¹⁹ We thus speculate that in our case the application of a positive voltage partially reduces the CoFeB layer, while preserving an interfacial oxidation condition, which maximizes the PMA contribution to K_{eff} . On the contrary, the application of a negative gate voltage drives oxygen into the CoFeB layer which further oxidizes this layer. This leads to a decrease of both M_S and interfacial PMA (i.e., an increase of $|K_{\text{eff}}|$) thus explaining the decrease of the slope of the MOKE loop taken after application of a negative voltage (blue curve in Fig. 3). According to our interpretation, the electrical modulation of the magnetic anisotropy observed in Pt and Ta capped CoFeB/GdO_x samples has the same physical origin, related to magneto-ionic effects. The CFB-Ta system with an in-plane easy axis in the “as-grown” state behaves similarly to the CFB-Pt system displaying PMA: a positive gate voltage strengthens the out-of-plane component of the anisotropy (i.e., increases the value of K_{eff}), while a negative gate voltage weakens it, regardless of the buffer layer/CoFeB interface.

In summary, we have demonstrated the existence of magneto-ionic effects in CoFeB/GdO_x systems with as-grown in-plane and perpendicular-to-plane easy axis, grown on top of Ta and Ta/Pt buffer layers, respectively. In both cases, we observe a decrease (increase) in the perpendicular to plane magnetic anisotropy when oxygen is driven into (out of) the CoFeB film via electrically induced migration of oxygen ions in GdO_x. For Pt/CoFeB/GdO_x stacks, a magneto-ionic mediated spin reorientation transition has been achieved by application of ± 2 V, associated with an interface magnetic anisotropy energy variation greater than 0.2 mJ m^{-2} . In the case of Ta/CoFeB/GdO_x structures, a sizable electrical modulation of the CoFeB magnetic properties has been achieved, but the magnetic anisotropy remains in-plane for applied voltages up to ± 10 V.

See [supplementary material](#) for measurements of uni-axial in-plane anisotropy in CFB-Ta multilayers, comparison between CFB-Pt and CFB-Ta samples with identical CoFeB thickness, multiple switching, and thermodynamic considerations.

We gratefully acknowledge skillful technical support from D. Bono. This work was partially funded by the Samsung Global MRAM Innovation program. L.B. acknowledges funding from Fondazione Roberto Rocca. R. B. acknowledges financial support from Fondazione Cariplo via the project Magister (Project No. 2013-0726).

¹D. E. Nikonov and I. A. Young, *IEEE J. Explor. Solid-State Comput. Devices Circuits* **1**, 3 (2015).

²M. Bibes, *Nat. Mater.* **11**, 354 (2012).

³C. Chappert, A. Fert, and F. N. Van Dau, *Nat. Mater.* **6**, 813 (2007).

⁴F. Matsukura, Y. Tokura, and H. Ohno, *Nat. Nanotechnol.* **10**, 209 (2015).

⁵J. W. Lee, S. C. Shin, and S. K. Kim, *Appl. Phys. Lett.* **82**, 2458 (2003).

⁶S. K. Kim, J. W. Lee, S. C. Shin, H. W. Song, C. H. Lee, and K. No, *J. Magn. Magn. Mater.* **267**, 127 (2003).

- ⁷M. Weisheit, S. Fähler, A. Marty, Y. Souche, C. Poinignon, and D. Givord, *Science* **315**, 349 (2007).
- ⁸C. A. F. Vaz, *J. Phys.: Condens. Matter* **24**, 333201 (2012).
- ⁹G. Radaelli, D. Petti, E. Plekhanov, I. Fina, P. Torelli, B. R. Salles, M. Cantoni, C. Rinaldi, D. Gutiérrez, G. Panaccione, M. Varela, S. Picozzi, J. Fontcuberta, and R. Bertacco, *Nat. Commun.* **5**, 3404 (2014).
- ¹⁰M. Bibes and A. Barthélémy, *Nat. Mater.* **7**, 425 (2008).
- ¹¹W.-G. Wang, M. Li, S. Hageman, and C. L. Chien, *Nat. Mater.* **11**, 64 (2012).
- ¹²M. Asa, L. Baldrati, C. Rinaldi, S. Bertoli, G. Radaelli, M. Cantoni, and R. Bertacco, *J. Phys.: Condens. Matter* **27**, 504004 (2015).
- ¹³L. Baldrati, C. Rinaldi, A. Manuzzi, M. Asa, L. Aballe, M. Foerster, N. Biškup, M. Varela, M. Cantoni, and R. Bertacco, *Adv. Electron. Mater.* **2**, 1600085 (2016).
- ¹⁴D. B. Strukov, G. S. Snider, D. R. Stewart, and R. S. Williams, *Nature* **453**, 80 (2008).
- ¹⁵B. Govoreanu, G. S. Kar, Y. Y. Chen, V. Paraschiv, S. Kubicek, A. Fantini, I. P. Radu, L. Goux, S. Clima, R. Degraeve, N. Jossart, O. Richard, T. Vandeweyer, K. Seo, P. Hendrickx, G. Pourtois, H. Bender, L. Altimime, D. J. Wouters, J. A. Kittl, and M. Jurczak, *Tech. Dig.-Int. Electron Devices Meet.* **2011**, 729.
- ¹⁶U. Bauer, S. Emori, and G. S. D. Beach, *Appl. Phys. Lett.* **100**, 192408 (2012).
- ¹⁷U. Bauer, S. Emori, and G. S. D. Beach, *Nat. Nanotechnol.* **8**, 411 (2013).
- ¹⁸U. Bauer, L. Yao, A. J. Tan, P. Agrawal, S. Emori, H. L. Tuller, S. Van Dijken, and G. S. D. Beach, *Nat. Mater.* **14**, 174 (2015).
- ¹⁹C. Bi, Y. Liu, T. Newhouse-Illige, M. Xu, M. Rosales, J. W. Freeland, O. Mryasov, S. Zhang, S. G. E. Te Velthuis, and W. G. Wang, *Phys. Rev. Lett.* **113**, 267202 (2014).
- ²⁰S. Ikeda, J. Hayakawa, Y. Ashizawa, Y. M. Lee, K. Miura, H. Hasegawa, M. Tsunoda, F. Matsukura, and H. Ohno, *Appl. Phys. Lett.* **93**, 082508 (2008).
- ²¹S. S. P. Parkin, C. Kaiser, A. Panchula, P. M. Rice, B. Hughes, M. Samant, and S.-H. Yang, *Nat. Mater.* **3**, 862 (2004).
- ²²S. Ikeda, K. Miura, H. Yamamoto, K. Mizunuma, H. D. Gan, M. Endo, S. Kanai, J. Hayakawa, F. Matsukura, and H. Ohno, *Nat. Mater.* **9**, 721 (2010).
- ²³E. Albisetti, D. Petti, M. Pancaldi, M. Madami, S. Tacchi, J. Curtis, W. P. King, A. Papp, G. Csaba, W. Porod, P. Vavassori, E. Riedo, and R. Bertacco, *Nat. Nanotechnol.* **11**, 545 (2016).
- ²⁴S. Y. Jang, C.-Y. Y. You, S. H. Lim, and S. R. Lee, *J. Appl. Phys.* **109**, 13901 (2011).
- ²⁵J. Stöhr, *J. Magn. Magn. Mater.* **200**, 470 (1999).
- ²⁶M. T. Johnson, P. J. H. Bloemen, F. J. A. Den Broeder, and J. J. De Vries, *Rep. Prog. Phys.* **59**, 1409 (1996).
- ²⁷H. E. Nigh, S. Legvold, and F. H. Spedding, *Phys. Rev.* **132**, 1092 (1963).
- ²⁸D. R. Lide, *CRC Handbook of Chemistry and Physics* (CRC Press, 2013).